International Journal of Thermophysics, Vol. 26, No. 4, July 2005 (© 2005)
DOI: 10.1007/s10765-005-6721-9

Rectangular Wires in Pulse-Heating Experiments[1]

G. Lohöfer[2,3] and G. Pottlacher[4]

The electric and temperature fields in a pulse-heated wire with a quadratic cross section are calculated analytically. The quick increase of the current through the wire during the pulse-heating process results in a nonuniform electric field (skin effect), and thus also a nonuniform temperature field over the wire cross section. By means of a typical pulse-heating experiment performed on a quadratic niobium wire, the magnitudes of the deviations of these fields from their mean values are graphically displayed. Compared with the strength of the mean fields, these deviations are significant only in the first few μs of the heating process.

KEY WORDS: exploding wire; nonuniform electric field; nonuniform temperature field; pulse heating; rectangular cross section.

1. INTRODUCTION

For the determination of thermophysical properties of metals at temperatures between ca. 1000 and 7000 K, the fast ohmic pulse-heating technique can be applied [1]. This method generally uses wire-shaped metal samples of ca. 0.5 mm diameter and 60 mm length which, as part of a fast capacitor discharge apparatus, are very rapidly resistively volume heated and melted with heating rates of about $10^7\ \mathrm{K \cdot s^{-1}}$. Therefore, this ohmic pulse-heating technique is also known as the "exploding wire technique" in the older literature. Thermophysical data obtained by fast pulse heating are very reliable due to improved data acquisition systems and are often used for numerical simulations.

[1] Paper presented at the Seventh International Workshop on Subsecond Thermophysics, October 6–8, 2004, Orléans, France.
[2] Institute of Space Simulation, DLR German Aerospace Center, 51170 Köln, Germany.
[3] To whom correspondence should be addressed. E-mail: Georg.Lohoefer@dlr.de
[4] Institute of Experimental Physics, TU Graz, 8010 Graz, Austria.

During the electric discharge through the solid and, after melting, liquid metal specimen measurements of the current through the wire, the voltage drop along the wire, the radiance temperature, and the thermal expansion of the wire are performed as a function of time. Then, via simple physical relations, the heat capacity, enthalpy, electrical resistivity, density, thermal conductivity, and thermal diffusivity for the solid and liquid samples and their dependence on temperature can be calculated from these measurement results. However, these relations implicitly assume uniform electric fields and current densities over the wire cross section and thus also homogeneously heated samples despite the fact, that, according to Faraday's law, quick changes of electric fields, which occur in fast pulse-heating experiments, result in additional induction fields and eddy currents disturbing any spatial uniformity. On the other hand, detailed calculations about the influence of the skin effect during fast pulse heating [2] show that variations of the electric field, which are significant compared to the mean field, generally occur only at the beginning of the heating process. Variations of the temperature field across the wire, which result from ohmic losses of the nonuniform current density field driven by the electric field, remain however, because the equalizing effect of the heat conduction is negligibly small within the very short experimental time. But, compared to the absolute temperatures of the high melting metals under investigation, these temperature variations are, in general, relatively small, as we will show in the following.

Since many pure metals and metallic alloys are ductile, the wire-shaped samples, used for the pulse-heating experiment, are generally manufactured by drawing. This technique has the advantage of simplicity, and it enables the formation of elementary, circular cross sections of appropriate and constant diameters over the whole length of the wire. Recently however, the industry is interested in thermophysical data of materials like TiAl intermetallic alloys [3], which possess attractive high-temperature mechanical properties. But, due to their weakness and limited ductility, the manufacturing of wire samples from these materials has to be done by cutting from the bulk by spark erosion, resulting in rectangular wire cross sections.

The altered shape of the cross section immediately brings up questions on what the current densities and temperature distributions in the rectangular pulse-heated wire will be and how homogeneous these fields are, especially in the four corners of the sample. As already mentioned above, the answers have direct implication on the temperature measurement and the determination of thermophysical material pararmeters. These problems are investigated in this paper.

2. EXPERIMENTAL ARRANGEMENT

The experimental situation is schematically shown in Fig. 1. A wire-shaped sample of a quadratic cross section, the half-thickness $a(\approx 0.2\,\text{mm})$ of which is much smaller than its length $l(\approx 60\,\text{mm})$, is fixed along the axis of a cylindrical experimental chamber of internal radius $b(\approx 75\,\text{mm})$ and wall thickness $d(\approx 3\,\text{mm})$. Thus, we have the geometric relations,

$$a \ll l, \quad d \ll l \tag{1}$$

and

$$a \ll b. \tag{2}$$

These relations simplify the following calculations considerably, because we may neglect all terms of the order of magnitude of a/l, d/l, and a/b.

3. ELECTRIC FIELDS

3.1. Partial Differential Equations

A time-dependent voltage source $U(t)$, generally a condenser bank of high capacity, feeds a current $I(t)$ into the electric circuit consisting of the wire sample and the chamber walls. The resulting space- and time-dependent electric field $\mathbf{E}(\mathbf{x}, t)$ and current density field $\mathbf{j}(\mathbf{x}, t)$ in the wire and the surrounding area are sufficiently well described by the partial differential equation [4],

$$\Delta \mathbf{E}(\mathbf{x}, t) = \mu_0 \partial/\partial t\, \mathbf{j}(\mathbf{x}, t) + \nabla \rho(\mathbf{x}, t)/\varepsilon_0, \tag{3}$$

which results from the quasi-stationary Maxwell equations, in which the displacement current term is neglected, and Ohm's law,

$$\mathbf{j}(\mathbf{x}, t) = \sigma(\mathbf{x}, t)\mathbf{E}(\mathbf{x}, t). \tag{4}$$

Here $\sigma(\mathbf{x}, t)$ denotes the electrical conductivity and $\rho(\mathbf{x}, t)$ is the electrical charge density. In the following we assume for the sake of simplicity:

1. $\sigma(\mathbf{x}, t) = \sigma_0$ to be constant (temperature independent) inside the conductors.

According to the experimental arrangement shown in Fig. 1 and Eq. (4),

2. only the z-component of the electric field is of interest,

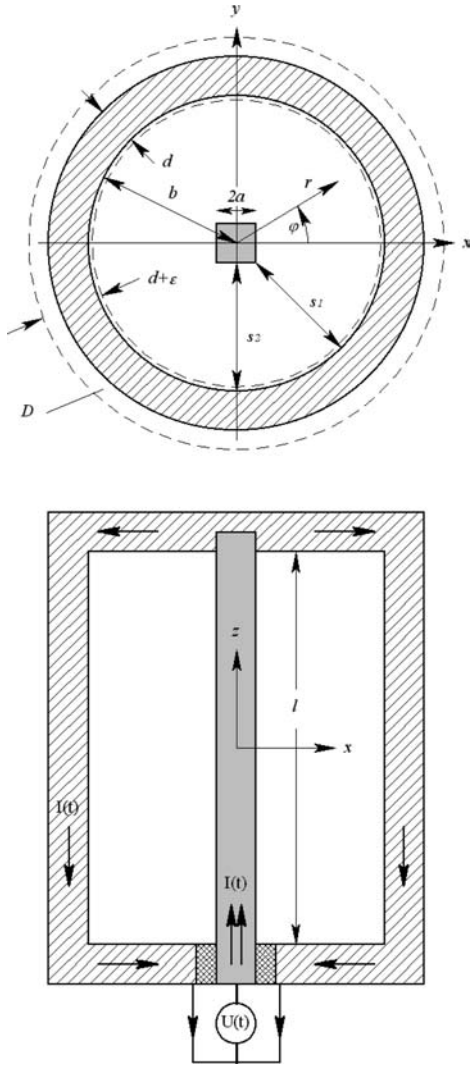

Fig. 1. (a) Schematic view on the cut along the x-, y-plane (z = 0) through the experimental arrangement. (b) Schematic view on the cut along the x-, z-plane (y = 0) through the experimental arrangement. A pulse-heated wire of quadratic cross section (gray), powered by a time-dependent voltage source $U(t)$, is fixed in the center of a cylindrical experimental chamber of electrically conducting (hatched) and nonconducting (cross-hatched) walls. The displayed dimensions are not in correct scale.

because this component alone drives the current through the wire and the surrounding cylinder jacket. Thus, writing "electric field," we only mean its z-component in the following.

Inside the thin wire and the cylinder jacket the characteristic length scale of field variations perpendicular to the z-direction is determined by a or d, i.e., $|\mathbf{e}_z \times \nabla| \approx 1/a$ or $\approx 1/d$, respectively, whereas for field variations in the z-direction, it is generally given by l, i.e., $|\partial/\partial z| \approx 1/l$. Consequently, due to Eq. (1), gradients in the z-direction, and therefore

3. any dependence of the fields on the z-variable in the wire and the cylinder jacket, can be disregarded.

Thus, for the z-component of electric and current density fields in the conductors, defined by

$$E_z(x, y, t) := \mathbf{E}(\mathbf{x}, t) \cdot \mathbf{e}_z \text{ and } j_z(x, y, t) := \mathbf{j}(\mathbf{x}, t) \cdot \mathbf{e}_z,$$

Eqs. (3) and (4) now read in Cartesian coordinates (x, y, z),

$$\left\{ \frac{\partial^2}{\partial x^2} + \frac{\partial^2}{\partial y^2} \right\} E_z(x, y, t) = \mu_0 \frac{\partial}{\partial t} j_z(x, y, t), \tag{5}$$

$$j_z(x, y, t) = \sigma_0 E_z(x, y, t). \tag{6}$$

In the area between the wire and outer cylinder jacket, where neither electric currents nor electric charges are present, the partial differential equation, Eq. (3), reads for the z-component of the electric field in cylindrical coordinates (r, φ, z),

$$\left\{ \frac{1}{r} \frac{\partial}{\partial r} r \frac{\partial}{\partial r} + \frac{1}{r^2} \frac{\partial^2}{\partial \varphi^2} + \frac{\partial^2}{\partial z^2} \right\} E_z(r, \varphi, z, t) = 0. \tag{7}$$

3.2. Boundary Conditions

In order to solve Eqs. (5) and (6) for the electric field inside the wire, we need to know the field at the wire boundary. This is provided by the solution of Eq. (7) yielding the electric field between the wire and the surrounding cylinder. But also the solution of Eq. (7) requires boundary values at the inner surface of the cylinder jacket. These will be calculated as follows.

Denoting by the index W quantities belonging to the wire and by the index C those belonging to the cylinder jacket, we estimate for the mean values $\langle E_z \rangle$ and $\langle j_z \rangle$ of the electric and current density fields inside these

conductors that

$$-\langle E_z\rangle_C = \frac{-\langle j_z\rangle_C}{\sigma_C} \approx \frac{1}{\sigma_C}\frac{-I_C}{2\pi bd} = \frac{\langle j_z\rangle_W}{\sigma_C}\frac{4a^2}{2\pi bd} = \frac{\sigma_W}{\sigma_C}\frac{4a}{2\pi d}\frac{a}{b}\langle E_z\rangle_W,$$

where Eq. (6), and the fact that the total currents through the wire and the jacket satisfy $I_W = -I_C$, have been used. Hence, according to Eq. (2), $|\langle E_z\rangle_C| \ll |\langle E_z\rangle_W|$. Being mainly interested in the field inside the wire, this permits us to set the electric field inside the jacket to zero. Due to the continuity of the tangential component E_z everywhere at the inner jacket surface, which we note here without proof, we find as the first boundary condition of Eq. (7) at $r = b$,

$$\lim_{\substack{r\to b\\ r<b}} E_z(r,\varphi,t) = 0. \tag{8}$$

The determination of the second condition is influenced by the following considerations.

The time-dependent change of the electrical current density through the wire influences by magnetic induction also the electric and current density fields in the cylinder jacket. This means, that, due to the rectangular cross section of the wire, the fields in the circular cylinder jacket are, strictly speaking, not axially symmetric. But, since the magnetic field decreases as $B(s) \propto s^{-1}$ with the distance s from a current line [4], the relative difference of the magnetic field and thus also of the electric and current density field in the cylinder jacket between the two extremes s_1 and s_2, shown in Fig. 1, can be estimated by

$$\frac{B(s_1) - B(s_2)}{B(s_1)} = 1 - \frac{b - a\sqrt{2}}{b-a} = \frac{\sqrt{2}-1}{1-a/b}\cdot\frac{a}{b} \ll 1,$$

where Eq. (2) has been used. Consequently,

4. for radial distances $r \geq b$ from the wire axis, the fields can be regarded as rotationally symmetric.

The second boundary condition follows from an integration of Eq. (5) over the annulus D of thickness $d+\varepsilon$ with $\varepsilon > 0$, bounded by the dashed lines in Fig. 1. Since, according to the above result, the φ-dependence of E_z can be neglected near $r = b$ as well as the z-dependence due to condition 3, this integral reads in cylindrical coordinates (r, φ),

$$0 = \int_0^{2\pi}\int_b^{b+d+\varepsilon} \frac{1}{r}\frac{\partial}{\partial r} r \frac{\partial}{\partial r} E_z(r,t) r\, dr\, d\varphi$$
$$-\mu_0 \frac{\partial}{\partial t}\int\int_D j_z(r,t)\, dS = 2\pi \left[r \frac{\partial E_z(r,t)}{\partial r}\right]_{r=b}^{r=b+d+\varepsilon} + \mu_0 \dot{I}(t),$$

where $I(t)$ denotes the total current through the wire and through the cylinder jacket and $\dot{I}(t)$ is its time derivative. Since the electric field disappears everywhere outside the experimental chamber including the outer boundary of D, which we note here without proof, the above equation leads immediately to the second boundary condition of Eq. (7) at $r = b$,

$$\lim_{\substack{r \to b \\ r < b}} \frac{\partial E_z(r, \varphi, t)}{\partial r} = \frac{\mu_0}{2\pi b} \dot{I}(t). \tag{9}$$

3.3. Electric Field between Wire and Cylinder Jacket

The electrical field between the wire and the cylinder jacket is the solution of the partial differential equation, Eq. (7), subjected to the boundary conditions, Eqs. (8) and (9). The simple, unique result reads

$$E(r, \varphi, t) = \frac{\mu_0}{2\pi} \dot{I}(t) \ln\left(\frac{r}{b}\right) \equiv \frac{\mu_0}{2\pi} \dot{I}(t) \ln\left(\frac{\sqrt{x^2 + y^2}}{b}\right) \tag{10}$$

and is displayed in Fig. 2. The field is negative and decreases steeply towards the tiny wire. Evidently, the boundary conditions have transferred the rotational symmetry to the electric field in the whole area outside the wire.

Only for interest, we finally note that the radial component of the electric field that drives the current in the top and bottom of the cylindrical experiment chamber enters also into the area between the cylinder jacket and the wire. Here it starts and ends on influenced electric charges on the metal surfaces, but it does not enter the wire and the cylinder jacket itself.

3.4. Electric Field in the Quadratic Wire

The combination of Eqs. (5) and (6) results in the partial differential equation for the interesting z-component of the electric field in the rectangular wire;

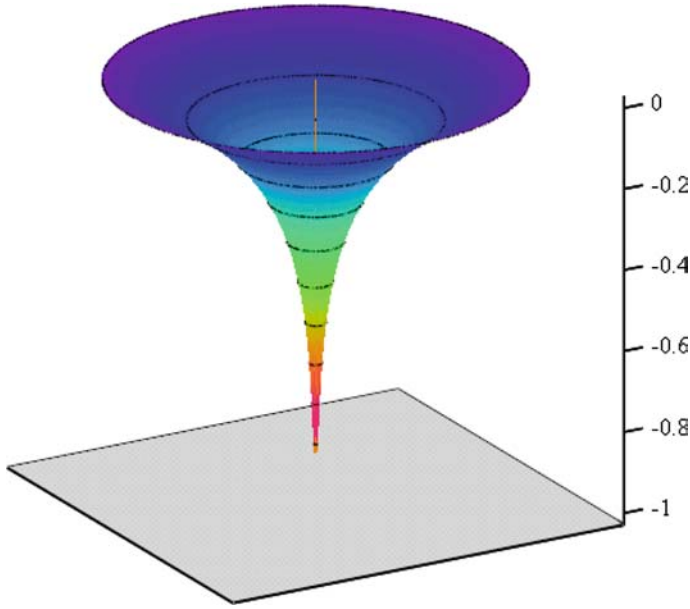

Fig. 2. z-component of the normalized electric field between the wire and the surrounding circular cylinder jacket. The field decreases steeply from zero at the inner jacket surface towards negative values at the wire surface. The wire is displayed by the tiny line in the center.

$$\left\{\frac{\partial^2}{\partial\xi^2}+\frac{\partial^2}{\partial\eta^2}\right\}E_z(\xi,\eta,\tau)=\frac{\partial}{\partial\tau}E_z(\xi,\eta,\tau), \tag{11}$$

where the following dimensionless variables have been introduced:

$$\xi:=\frac{x}{a},\quad \eta:=\frac{y}{a},\quad \tau:=\frac{t}{a^2\mu_0\sigma_0}. \tag{12}$$

To find the corresponding boundary conditions, we note without proof that the derivative of $E_z(\xi,\eta,\tau)$ normal to the wire boundary is continuous at the wire boundary. This means, that from the derivative of Eq. (10) in the ξ-direction, we receive at the wire boundaries: $\xi=\pm1$, $-1<\eta<+1$ the relation,

$$\lim_{\substack{\xi\to\pm1\\|\xi|<1}}\frac{\partial E_z(\xi,\eta,\tau)}{\partial\xi}=\pm\frac{R_0}{l}\dot{I}(\tau)\frac{2/\pi}{1+\eta^2}, \tag{13a}$$

and from the derivative of Eq. (10) in the η-direction, we receive at the wire boundaries: $\eta = \pm 1, -1 < \xi < +1$ the relation,

$$\lim_{\substack{\eta \to \pm 1 \\ |\eta|<1}} \frac{\partial E_z(\xi, \eta, \tau)}{\partial \eta} = \pm \frac{R_0}{l} \dot{I}(\tau) \frac{2/\pi}{1+\xi^2}, \tag{13b}$$

where

$$R_0 := \frac{l}{4a^2\sigma_0}$$

is the Ohm resistance of the whole wire, and where now: $\dot{I}(\tau) := \partial/\partial\tau I(\tau)$. As the initial condition, we assume

$$I(\tau) = 0 \quad \Rightarrow \quad E_z(\xi, \eta, \tau) = 0 \quad \text{for } \tau = 0. \tag{14}$$

The z-component of the electric field in the quadratic wire now results from the unique solution of Eqs. (11), (13a), (13b), and (14). Expanded in a double Fourier series [5], it reads

$$\begin{aligned} &E_z(\xi, \eta, \tau) \\ &= \frac{R_0}{l}\Bigg(I(\tau) + \sum_{m=0}^{\infty} \sum_{\substack{n=0 \\ n+m\neq 0}}^{\infty} (2-\delta_{m,0})(2-\delta_{n,0})(-1)^{m+n+1} \frac{\alpha_m + \alpha_n}{2} h_{m,n}(\tau) \\ &\qquad \cos(m\pi\xi)\cos(n\pi\eta)\Bigg) \end{aligned} \tag{15}$$

with the time-dependent function,

$$\begin{aligned} h_{m,n}(\tau) &:= \int_0^\tau \dot{I}(\tau') \exp\Big[-(m^2+n^2)\pi^2(\tau-\tau')\Big] d\tau' \\ &\equiv I(\tau) - (m^2+n^2)\pi^2 \int_0^\tau I(\tau') \exp\Big[-(m^2+n^2)\pi^2(\tau-\tau')\Big] d\tau', \end{aligned} \tag{16}$$

where the second term results from partial integration of the first one, the definition,

$$\alpha_k := (-1)^{k+1} \frac{4}{\pi} \int_0^1 \frac{\cos(k\pi t)}{1+t^2} dt \tag{17}$$

and the Kronecker delta,

$$\delta_{i,k} := \begin{cases} 1 & \text{if} \quad i = k \\ 0 & \text{if} \quad i \neq k \end{cases}. \tag{18}$$

Evidently, the stationary value of E_z,

$$E_{z,\mathrm{stat}}(\tau) := \frac{R_0}{l} I(\tau), \tag{19}$$

which is identical to the mean value of E_z over the wire cross section, is just given by the first term in Eq. (15). The second term in Eq. (15) describes the spatial deviation from this uniform value in case of a changing electric current, i.e., if $\dot{I}(\tau) \neq 0$.

3.5. Special Case: Electric Field in a Pulse-Heated Quadratic Niobium Wire

A typical current-time diagram $I(\tau)$, measured for a pulse-heated circular niobium wire of 0.5 mm diameter [6], is shown in Fig. 3. We use this diagram to calculate in the following with Eqs. (15)–(18) the electric field in a quadratic niobium wire of the same cross-sectional area, which corresponds to a wire thickness of $2a \approx 0.44$ mm. The electrical conductivity of the wire material, assumed to be constant in the present theory, is set to $\sigma_0 = 2.97 \times 10^6\ \Omega^{-1} \cdot \mathrm{m}^{-1}$, which corresponds to the electrical conductivity of niobium at ca. 700 K. With these values the heating time to reach the melting temperature in the solid quadratic niobium wire, calculated from Eq. (23), agrees just with the measured one; see Fig. 3.

In Fig. 4, electric field distributions over the quadratic wire cross section, i.e., for $-a \leq x \leq a$ and $-a \leq y \leq a$, of our above defined example are displayed at the times $t = 0.8\,\mu\mathrm{s}$, $t = 4\,\mu\mathrm{s}$, and $t = 26\,\mu\mathrm{s}$ after the current has been switched on. In the left column of Fig. 4, the absolute deviation of the electric field from its stationary value, i.e., $E_z(x, y, t) - E_{z,\mathrm{stat}}(t)$, is presented. According to Eqs. (15), (16), and (19) this quantity depends only on the time derivative of the current. For increasing current, occurring at $t = 0.8\,\mu\mathrm{s}$ and $t = 4\,\mu\mathrm{s}$, the field shows the well known skin effect, i.e., it is lower in the center of the wire than on its surface. For decreasing current, occurring at $t = 26\,\mu\mathrm{s}$, this behavior is just inverted. Furthermore, we see that $E_z(x, y, t) - E_{z,\mathrm{stat}}(t)$ is in the corners of the quadratic wire about 30% higher than in the middle of the side surfaces.

As already mentioned in the introduction, thermophysical properties are generally calculated from the data of a pulse-heating experiment under the assumption of a homogeneous electric field within the wire specimen. The error accepted hereby depends on the relative deviation of the actual electric field from its stationary value: $[E_z(x, y, t) - E_{z,\mathrm{stat}}(t)]/E_{z,\mathrm{stat}}(t)$. Due to the rapid increase of the current and thus, according to Eq. (19), also of $E_{z,\mathrm{stat}}(t)$, this quantity decreases however very quickly in the

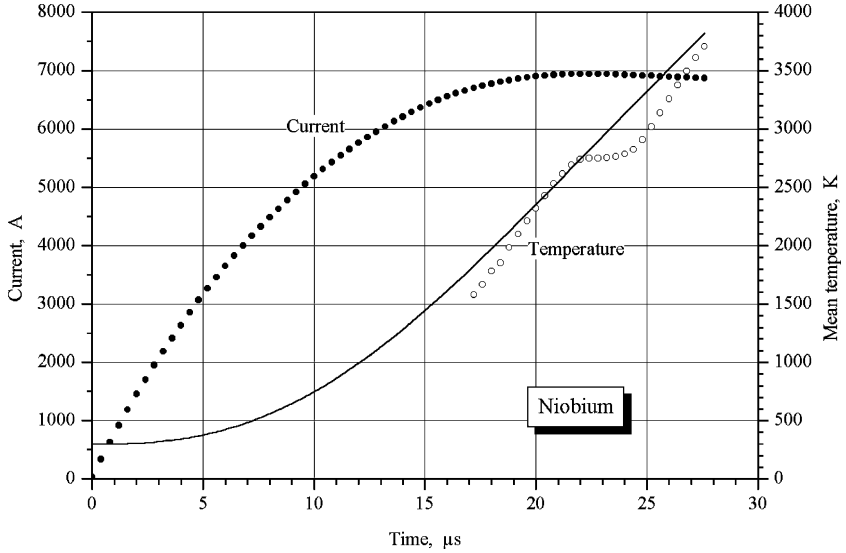

Fig. 3. Measured values of the electric current (closed dots) and of the temperature (open dots) in a pulse-heated circular niobium wire of 0.5 mm diameter. The calculated mean temperature of the corresponding quadratic wire of 0.44 mm thickness and $2.97 \cdot 10^6 \Omega^{-1} \cdot \mathrm{m}^{-1}$ electrical conductivity is represented by the full line.

course of time. For our special niobium specimen the relative field deviation, presented in the right column of Fig. 4, is below 5% after 0.8 μs and below 1% after 4 μs. Thus, a few μs after the beginning of the pulse-heating experiment, the assumption of a homogeneous field in the rectangular wire is generally justified.

Without proof, we finally note the simple, universally valid estimation,

$$\left| \frac{E_z(x, y, t) - E_{z,\mathrm{stat}}(t)}{E_{z,\mathrm{stat}}(t)} \right| \leq \frac{0.39}{\tau(t)} = 0.39 \frac{a^2 \mu_0 \sigma_0}{t}, \tag{20}$$

which holds for a typical pulse-heating experiment, where $\dot{I}(t) \geq 0$ and $\ddot{I}(t) \leq 0$, cf. Fig. 3.

4. TEMPERATURE FIELD

4.1. Temperature Field in the Quadratic Wire

The temperature field $T(x, y, t)$ in the pulse-heated wire is calculated from the energy-balance equation [7]. For constant (temperature-independent) material parameters, it reads in the dimensionless variables

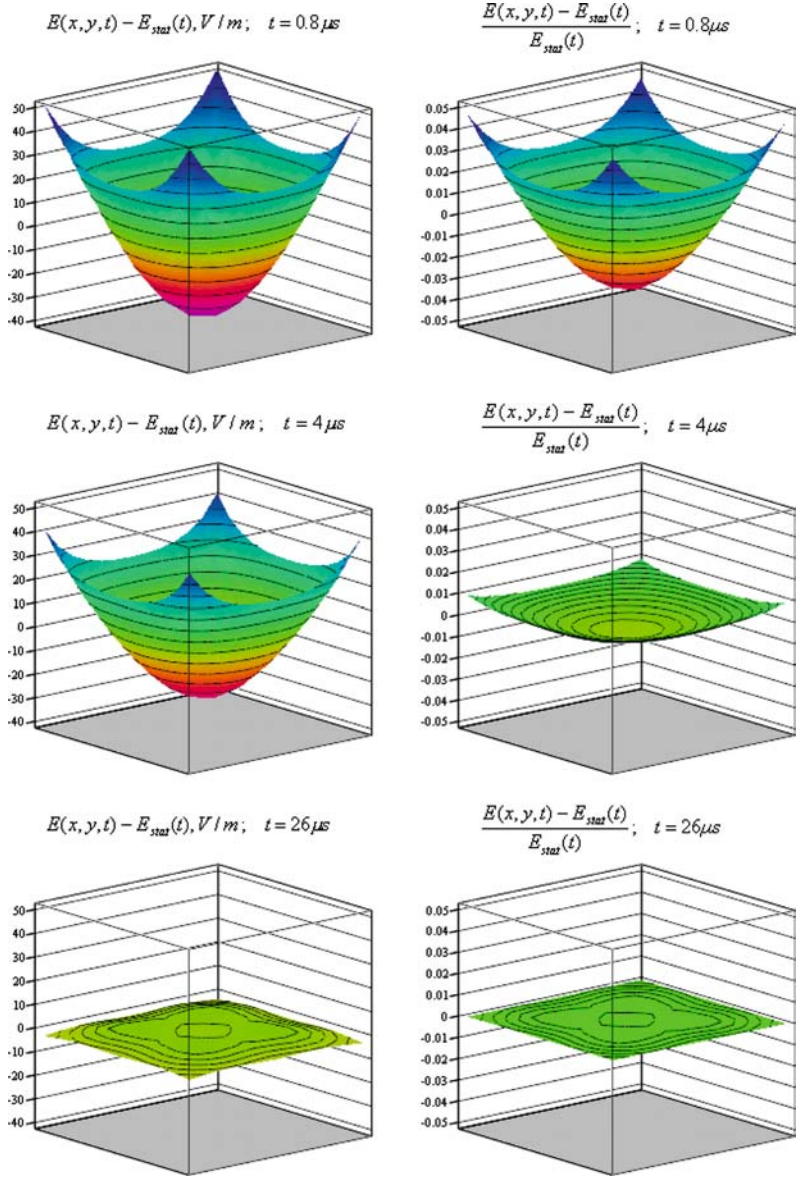

Fig. 4. Absolute (left) and relative (right) deviations of the electric field from its stationary value over the cross section of a quadratic pulse-heated niobium wire for different times after the heating current, shown in Fig. 3, has been switched on. For increasing current, the field shows the typical skin effect.

of Eq. (12),

$$\frac{\rho_m c_p}{a^2 \mu_0 \sigma_0}\left[\frac{\partial T(\xi,\eta,\tau)}{\partial \tau} - \kappa\left\{\frac{\partial^2}{\partial \xi^2}+\frac{\partial^2}{\partial \eta^2}\right\} T(\xi,\eta,\tau)\right]$$
$$= \sigma_0 E_z^2(\xi,\eta,\tau) - \delta(\mathbf{x}-\mathbf{x}_B) S(T(\mathbf{x}_B,\tau)) \tag{21}$$

and describes the increase of the internal-energy density in a volume element of the wire (first term on the left of Eq. (21)), caused by heat conduction from the surrounding elements (second term on the left), the power density input from the electric field (first term on the right), and the power density loss by radiation (second term on the right).

The last-mentioned term is the product of the Dirac delta function $\delta(\mathbf{x}-\mathbf{x}_B)$ and the Stefan-Boltzmann radiation law $S(T(\mathbf{x}_B,\tau))$ [7] and depends on the coordinates of the wire boundary $\mathbf{x}_B := (\xi_B, \eta_B)$ only. During the fast pulse heating, shown in Fig. 3, this term is, however, much smaller (for niobium at 4000 K by a factor 10^{-4}) than the term describing the electric power density input. Hence, we assume in the following that

5. heat loss by radiation can generally be neglected.

The order of magnitude of the heat conduction term in Eq. (21) is determined by the material specific quantity,

$$\kappa := \frac{\lambda \mu_0 \sigma_0}{\rho_m c_p},$$

where ρ_m, c_p, and λ denote the mass density, specific heat, and thermal conductivity of the wire material, respectively. For all metals above room temperature, $\kappa < 10^{-2}$. For niobium, we even have $\kappa < 4 \times 10^{-4}$. Accordingly, we assume in the following that

6. heat conduction can generally be neglected, when pulse heating lasts only a few τ.

Under these conditions the remaining two terms of Eq. (21) can immediately be integrated leading to the temperature field,

$$T(\xi,\eta,\tau) = \frac{a^2 \mu_0 \sigma_0^2}{\rho_m c_p}\int_0^\tau E_z^2(\xi,\eta,\tau')d\tau' + T_0 \tag{22}$$

in the wire where T_0 is the uniform temperature at $\tau = 0$. Another important quantity represents the mean temperature in the quadratic wire;

$$\langle T\rangle(\tau) = \tfrac{1}{4a^2}\int_{-a}^{+a}\int_{-a}^{+a} T(x,y,\tau)\,dx\,dy = \tfrac{a^2\mu_0\sigma_0^2}{\rho_m c_p}\int_0^\tau\int_0^1\int_0^1 E_z^2(\xi,\eta,\tau')\,d\xi\,d\eta d\tau' + T_0$$
$$= \tfrac{a^2\mu_0\sigma_0^2}{\rho_m c_p}\sum_{m=0}^{\infty}\sum_{n=0}^{\infty}\left\{(2-\delta_{m,0})(2-\delta_{n,0})\left(\tfrac{\alpha_m+\alpha_n}{2}\right)^2\int_0^\tau h_{n,m}^2(\tau')d\tau'\right\} + T_0 \tag{23}$$

where the integral over the wire cross section could be evaluated analytically. Evidently, the time integrals in both equations accumulate to the deviation of the temperature field from its mean value, i.e., $T(\xi, \eta, \tau) - \langle T \rangle(\tau)$, in the course of time.

4.2. Special Case: Temperature Field in a Pulse-Heated Quadratic Niobium Wire

On the basis of the measured current-time diagram of a niobium specimen displayed in Fig. 3, the electric field has been calculated for a quadratic wire of 0.44 mm thickness and a conductivity of $2.97 \times 10^6\ \Omega^{-1} \cdot m^{-1}$, which corresponds to the conductivity of niobium at ca. 700 K. The appropriate temperature-time behavior $\langle T \rangle(t)$, calculated with Eq. (23), is shown by the solid line in Fig. 3. It agrees at the melting temperature with the measured value. Disregarding the melting plateau, the remaining deviations between measurement and calculation are caused by the assumption of a constant (temperature-independent) electrical conductivity.

For the same situation Fig. 5 presents the calculated deviations of the temperature field from its mean value, i.e., $T(x, y, t) - \langle T \rangle(t)$, at the times $t = 6\,\mu s$, $t = 14\,\mu s$, $t = 22\,\mu s$, and $t = 28\,\mu s$ after the current has been switched on. The results show that the deviations accumulate over the course of time. As in the case of the electric field, the temperature in the corners is about 30% higher than in the middle of the side surfaces. However, compared with the niobium melting temperature of 2740 K, reached after $t = 22\,\mu s$, see Fig. 3, the deviations of the temperature field from its mean value, which vary between -7 K in the center and $+10$ K in the corners of the quadratic wire, are relatively small.

5. SUMMARY

In this paper we calculated analytically the electric field and the temperature field in a pulse-heated wire of quadratic cross section. The quick increase of the current through the wire during the fast heating process (see the niobium example in Fig. 3) causes a nonuniform distribution (skin effect) of both fields over the wire cross section. Their deviations from the dedicated mean values are of main interest in this paper. The present calculations show that, in general, the electric and temperature fields are lower in the center of the wire than on its side surfaces, and on the side surfaces they are lower in the middle than in the corners. For a pulse-heated niobium wire this is exemplified in the left column of Fig. 4 and Fig. 5. However, compared with the strength of the mean fields, these deviations are significant only in the first few μs of the heating process,

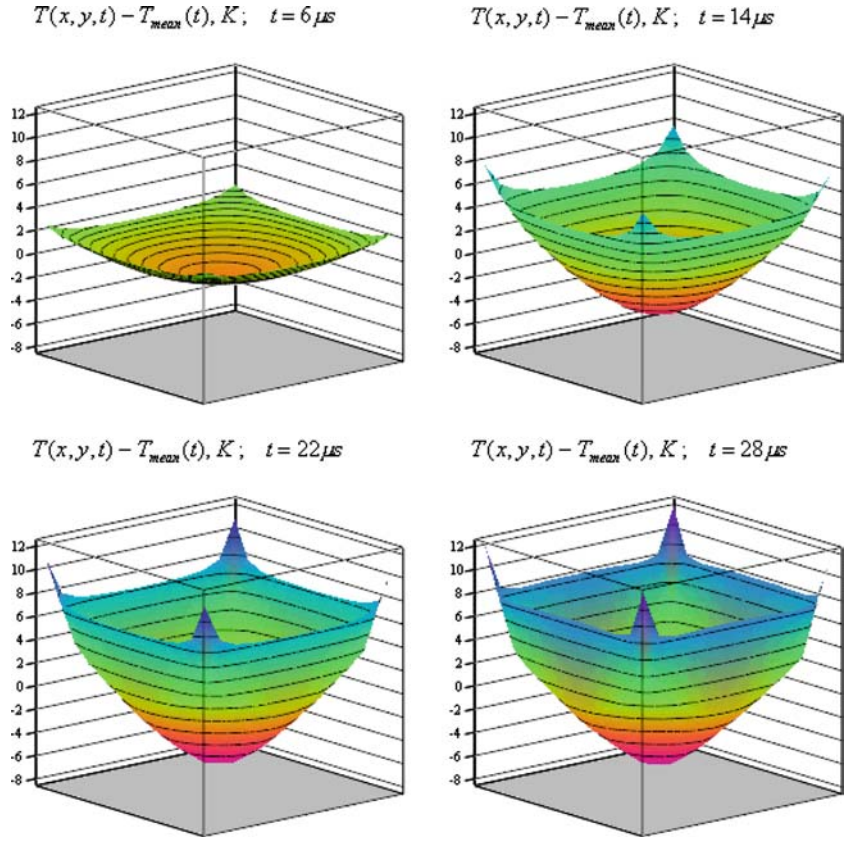

Fig. 5. Deviation of the temperature field from its mean value over the cross section of a quadratic pulse-heated niobium wire for different times after the heating current, shown in Fig. 3, has been switched on. The deviations increase over the course of time but are still much lower than the mean temperature.

see the right column of Fig. 4 and the estimation in Eq. (20). Consequently, if the first few μs of a pulse-heating experiment are disregarded, the error in the calculation of thermophysical properties of a wire specimen from the measurement data becomes negligibly small.

Although the simplifying assumption of a constant electrical wire conductivity led to errors in the calculation of the mean temperature-time development (see Fig. 3), it had, however, only minor impact on the calculation of the magnitude of field nonuniformities, considered mainly in this paper.

Although the power loss by radiation from the side surfaces of the wire is negligibly small compared with the total power input by the electric field during the fast pulse-heating process (see Section 4.1), it causes nevertheless a temperature drop at these surfaces. The strength of this temperature nonuniformity, which impacts the pyrometrical temperature measurement of the wire, depends sensitively on the magnitude of the heat supply from the bulk to the surface, which is, however, very small within the very short heating time; see Section 4.1. This problem should be taken care of, and the order of magnitude of this temperature drop should be estimated in the future.

ACKNOWLEDGMENTS

The research grant donated from the German Aerospace Center for the sabbatical stay of G. Lohöfer at the Institute of Experimental Physics, TU Graz is gratefully acknowledged. Furthermore, G. Lohöfer thanks C. Cagran and B. Wilthan from this institute for their support and hospitality.

REFERENCES

1. G. Pottlacher, H. Hosaeus, A. Seifter, and E. Kaschnitz, *Scandinavian J. Metallurgy* **31**:161 (2002).
2. G. Lohöfer, *Int. J. Thermophys.* **14**:471 (1993).
3. C. Cagran, B. Wilthan, G. Pottlacher, B. Roebuck, M. Wickins, and R. A. Harding, *Intermetallics* **11**:1327 (2003).
4. G. Lehner, *Elektromagnetische Feldtheorie* (Springer, Berlin, 1994).
5. E. A. González-Velasco, *Fourier Analysis and Boundary Value Problems* (Academic Press, San Diego, 1995).
6. C. Cagran and B. Wilthan, *private communication* (2004).
7. H. S. Carslaw and J. C. Jaeger, *Conduction of Heat in Solids* (Clarendon Press, Oxford, 1973).